Heliyon 10 (2024) e26384

Contents lists available at ScienceDirect

Heliyon

journal homepage: www.cell.com/heliyon

Research article

Induced knockdown of *Mg-odr-1* and *Mg-odr-3* perturbed the host seeking behavior of *Meloidogyne graminicola* in rice

Tushar K. Dutta [a,*], Voodikala S. Akhil [a], Artha Kundu [a], Manoranjan Dash [a], Victor Phani [b], Anil Sirohi [a], Vishal S. Somvanshi [a]

[a] *Division of Nematology, ICAR-Indian Agricultural Research Institute, New Delhi, 110012, India*
[b] *Department of Agricultural Entomology, Uttar Banga Krishi Viswavidyalaya (Majhian Campus), Balurghat, 733133, India*

ARTICLE INFO

Keywords:
Attraction
Repulsion
Chemotaxis index
Pluronic gel
Gene expression
Double-stranded RNA

ABSTRACT

Root-knot nematode *Meloidogyne graminicola* is one of the most destructive plant parasites in upland as well as direct seeded rice. As an integral part of nematode biology, host finding behavior involves perceiving and responding to different chemical cues originating from the rhizosphere. A sustainable management tactic may include retardation of nematode chemoreception that would impair them to detect and discriminate the host stimuli. Deciphering the molecular basis of nematode chemoreception is vital to identify chokepoints for chemical or genetic interventions. However, compared to the well-characterized chemoreception mechanism in model nematode *Caenorhabditis elegans*, plant nematode chemoreception is yet underexplored. Herein, the full-length cDNA sequences of two chemotaxis-related genes (*Mg-odr-1* and *Mg-odr-3*) were cloned from *M. graminicola*. Both the genes were markedly upregulated in the early developmental stages of *M. graminicola* suggesting their involvement in host finding processes. RNAi-induced independent knockdown of *Mg-odr-1* and *Mg-odr-3* caused behavioral aberration in second-stage juveniles of *M. graminicola* which in turn perturbed the nematodes' host finding ability and parasitic success inside rice roots. Additionally, nematodes' chemotactic response to different host root exudates, volatile and nonvolatile compounds was affected. Our results demonstrating the role of specific chemosensory genes in modulating *M. graminicola* host seeking behavior can enrich the existing knowledge of plant nematode chemoreception mechanism, and these genes can be targeted for novel nematicide development or *in planta* RNAi screens.

1. Introduction

Plant-parasitic nematodes (PPNs) are one of the most difficult crop pathogens to manage that globally inflict a heavy toll in major food crops amounting to more than 100 billion US$ economic loss [1]. Rice and wheat constitute the major staple diet of global population; >50% of global population consumes rice. Rice root-knot nematode *Meloidogyne graminicola* Golden & Birchfield is a substantial yield-declining factor in rice-wheat cropping systems in Asia due to the nematodes' shorter life span (19–27 days at 22–29 °C) and ability to complete multiple generations in a crop cycle. Apart from Asia, *M. graminicola* incidence has also been reported from Central and South America [2], and Europe [3], indicating its dissemination potential across the globe. In the root vascular cylinder, *M. graminicola* post-parasitic juvenile induces feeding cells (giant cells) which acts as the continual nutrient source

* Corresponding author.
E-mail address: nemaiari@gmail.com (T.K. Dutta).

https://doi.org/10.1016/j.heliyon.2024.e26384
Received 17 July 2023; Received in revised form 18 January 2024; Accepted 12 February 2024
Available online 17 February 2024

throughout its life cycle. Hyperplasia and hypertrophy of the surrounding cells of feeding site result in the gall formation at root tip and hinder further root development. Additionally, water and nutrient transport is disrupted across the root vasculature leading to the detriment of plant yield [4,5]. Owing to the globally changing climate, scarce water and ever-increasing shrinkage of arable lands, a noticeable shift in global agriculture is occurring from submerged conditions towards water-intensive paddy cultivation involving upland and direct seeded rice. Intriguingly, *M. graminicola* has become more destructive under this changing cultivation practices [6,7].

Chemoreception is the most significant sensory modality of PPNs for their survival because they respond to host-derived chemical cues commencing from migration in soil to inducing and maintaining a suitable feeding site in the root tissue. Deciphering the molecular intricacies of PPN sensory perception is vital to identify targets or chokepoints for chemical or genetic interventions. A novel management tactic may include PPNs with retarded chemosensation that are unable to detect and discriminate the host stimuli [8,9]. Notably, plants expressing the chemodisruptive peptides and neuropeptides that target PPN chemotaxis and neuromusculation process, perturbed nematode penetration and development in plant root in environmentally sustainable manner [10,11].

Unfortunately, compared to an exhaustive literature on chemosensory gene repertoire in the model nematode *Caenorhabditis elegans* [12], information on PPN chemotaxis regulatory genes is extremely limited. This may be attributed to the ease of performing genetic manipulation in *C. elegans* using laser ablation, microinjection or feeding of recombinant *E. coli* cells. By contrast, PPNs are recalcitrant to forward genetics screen because of their microscopic size, narrow stylet aperture and thinner cuticle. Nevertheless, use of RNAi as reverse genetics screen has been quite successful in PPNs [13]. Assuming that sensory neuroanatomy is conserved among PPNs and *C. elegans* [14], PPNs may chemo-orientate by using its amphid (head) and phasmid (tail) neurons to perceive root diffusates, food stimulants, food deterrents as well as sex pheromones.

The *C. elegans* genome encodes ~21 heterotrimeric G proteins (contain three different subunits α, β and γ), ~500–1000 membrane-bound G protein-coupled receptors (GPCRs), and ~34 guanylyl cyclases or GCYs (ligand-independent receptors). A fraction of these genes were characterized by behavioral screening of loss-of-function mutants, such as odorant (*odr1-10*) defective mutants, thermotaxis (*ttx*) defective mutants, chemotaxis (*che, tax2/4/6, gpa1-15, daf11*) defective mutants, osmotic avoidance (*osm9*) mutants, aerotaxis (*npr1*) defective mutants etc. Downstream of GPCR signaling two signal transduction pathways play important role in chemosensation: a cGMP-gated channel that uses cGMP as secondary messenger and another TRPV channel [15].

Earlier, in our laboratory we characterized *odr-1/3*, *tax-2/4* genes from *M. incognita* [16]. In addition, we identified a *flp18* GPCR in *M. graminicola* [17]. Advancing that research towards characterizing the chemotaxis-related genes in *M. graminicola* will augment the existing knowledge on PPN chemotaxis mechanism and will provide an impetus to basic understanding of plant-PPN interaction. In the current study, two chemosensory genes *Mg-odr-1* and *Mg-odr-3* were molecularly and functionally characterized from *M. graminicola*.

2. Materials and methods

2.1. Nematode culturing

The pure culture of *M. graminicola* was maintained in the fibrous root system of *Oryza sativa* L. cv. PB1121 in a net house. Egg masses extracted (by sterilized forceps under the microscope) from the galled roots were kept for hatching on double-layered tissue paper supported on a wire mesh, which was submerged in sterile tap water in a Petri dish [18]. Freshly-hatched second-stage pre-parasitic juvenile stages (preJ2s) were collected after 24–48 h. For developmental stage-specific chemotaxis gene transcription analyses, other life stages including post-parasitic J2s (postJ2), J3 and J4 mixed stages, young females and adult egg-laying females were dissected out from the infected root using sterilized forceps.

2.2. Plant material

Seeds of *O. sativa* cv. PB1121 were soaked in autoclaved water overnight followed by surface sterilization with 70% ethyl alcohol for 1 min and rinsed thrice in sterile water before putting in a Petri plate harboring a wet Whatman grade 1 filter paper for germination in an incubator at 28 °C. 4-5 day-old seedlings were included in infection bioassays.

Diffusates were collected from various host roots including rice (cv. PB1121), tomato (cv. Pusa Ruby), eggplant (cv. Pusa Purple Long), tobacco (cv. Petit Havana), wheat (cv. Sonalika), maize (cv. Buland), marigold (cv. Arpit), and mustard (cv. Pusa Jai Kisan). These plants were grown by hydroponics in Hoagland medium for a fortnight. Exudates were vacuum concentrated by 50-fold by following the previously described methods [7,18,19].

2.3. Bioinformatics analysis

Initially, the amino acid sequences of *C. elegans* olfactory proteins ODR-1 and ODR-3 were used as the query in WormBase Parasite database (https://parasite.wormbase.org/) against the translated nucleotide sequences of *M. graminicola*. Obtained sequences were further interrogated against the published *M. graminicola* genomic and transcriptomic resources [20,21]. Return sequences with highest scoring reciprocal BLAST hits (expect value – 0.0, highest bit score) were subjected to conserved domain analysis in InterProScan database (https://www.ebi.ac.uk/interpro/search/sequence/), NCBI CDD (https://www.ncbi.nlm.nih.gov/cdd/), FGENESH (http://www.softberry.com/) etc. Sequences that contained guanylyl cyclase and Gα domains were designated as *Mg-odr-1* and *Mg-odr-3*, respectively. Specific primers were designed for full-length sequence cloning of chemosensory genes.

2.4. RNA isolation from M. graminicola

Total RNA was extracted from pooled J2s using NucleoSpin® RNA kit (Macherey-Nagel) by following the kit instructions. RNA quantity and quality were assessed in a Nanodrop ND-1000 spectrophotometer (Thermo Fisher Scientific) and by resolving in 1.0 % (w/v) agarose gel. Approximately 400 ng of purified RNA was reverse-transcribed to first-strand cDNA by using a cDNA synthesis kit (Superscript VILO, Invitrogen) and stored at -20 °C for downstream use. For stage-specific qPCR analysis, RNA was isolated from different developmental stages of *M. graminicola* followed by reverse transcription to cDNA as explained earlier.

2.5. Full-length sequence cloning of chemosensory genes

Rapid amplification of cDNA ends (RACE)-PCR protocol was adopted for this purpose. 5′ and 3′-RACE-Ready cDNA was synthesized from the first-strand cDNA of *M. graminicola* using RACE cDNA amplification kit (Clontech, TaKaRa) by priming with oligo (dT) primer and Smart II A oligonucleotide as per the kit instructions. 5′- and 3′-RACE fragments were synthesized by employing antisense and sense gene-specific primers (GSP), respectively, together with universal primers. Generated amplicons were cloned into pGEM-T Easy vector (Promega) and Sanger sequenced. Upon obtaining the complete cDNA, a pair of primers was designed to validate the full-length sequence. Full-length cDNA sequences were submitted to NCBI GenBank repository. Primer details are given in Supplementary Table 1.

Full-length cDNA sequence was annotated using various tools including ExPASy translate tool (https://web.expasy.org/), NCBI ORF finder (https://www.ncbi.nlm.nih.gov/orffinder/), and FGENESH tool (https://www.softberry.com/). NetNGlyc 1.0 (https://services.healthtech.dtu.dk/services/NetNGlyc-1.0/) and NetOGlyc 4.0 (https://services.healthtech.dtu.dk/services/NetOGlyc-4.0/) webservers aided in searching N- glycosylated and O-glycosylated amino acid residues. Chemosensory gene sequences were aligned with their homologous/orthologous sequences from other species across the Phylum Nematoda using ClustalW sequence alignment tool (https://www.ebi.ac.uk/Tools/msa/). Phylogenetic trees corresponding to different candidate genes were constructed using MEGA6 tool. Maximum Likelihood method was used to predict the evolutionary history of different chemosensory genes and Tamura 3 parameter model was followed that employed a discrete Gamma distribution to correct the evolutionary rate differences between sites. Bootstrap consensus was inferred from 1000 replicates and tree branches corresponding to less than 70% bootstrap replicates were collapsed. Conserved motifs in different chemosensory genes and their homologues were predicted via MEME Suite v 5.5.5 (https://meme-suite.org/meme/) followed by functional annotation of motifs in HHpred tool (http://toolkit.tuebingen.mpg.de/hhpred).

2.6. Gene expression analysis

qPCR-based expression analysis was carried out in CFX96 PCR thermocycler machine (BioRad). qPCR reaction mixture (10 μL) contained 1.5 ng of cDNA template, 750 nM each of forward and reverse primers, and 5 μL of SYBR Green PCR master-mix aliquot (BioRad). qPCR amplification conditions constituted a hot start of 95 °C for 30 s, then 40 cycles of 95 °C for 10 s and 60 °C for 30 s. In addition, a melt curve program (95 °C for 15 s, 60 °C for 15 s, a slow ramp from 60 to 95 °C) was run to determine the amplification specificity. Quantification cycle (Cq) value for each replicate was obtained from CFX Maestro software (BioRad) and fold change in target gene expression was quantified by $2^{-\Delta\Delta Cq}$ method. *M. graminicola* housekeeping genes, *18S rRNA* and actin [22], were used as the reference genes. At least three biological and three technical replicates were used for each samples. qPCR efficiency of primers was determined by constructing a standard curve (in which Cq values were plotted against cDNA concentration) from five-fold dilution series of nematode cDNA and then calculating the slope from a linear regression equation: $E = (10^{(-1/\text{slope})} - 1) \times 100$. Primer details and qPCR reaction efficiency are provided in Supplementary Table 2.

2.7. Designing and synthesis of double-stranded RNA (dsRNA) molecules

Firstly, target dsRNA regions (~400–500 bp target length are optimum for slicing of dsRNA into smaller siRNA molecules via RNaseIII or Dicer enzyme) were selected using different *in silico* tools including dsCheck (https://dscheck.rnai.jp/), siDirect tool (https://sidirect2.rnai.jp/), and Dharmacon webserver (https://horizondiscovery.com/). By scanning across the whole target dsRNA, the *in silico* tools predict siRNA generation probabilities. Additionally, probable off-target sites can be examined by analyzing the sequence homology of generated siRNAs with the siRNA database of related and non-target animals and plants. Sequences corresponding to target dsRNA were PCR-amplified from *M. graminicola* cDNA template and cloned into pGEM-T vector via TA cloning method. Primer details are provided in Supplementary Table 2.

Targeted dsRNA regions were PCR amplified from the recombinant pGEM-T vector using M13 primer pairs. Gel-purified PCR products were used as the template to generate sense and antisense RNA strands of each target gene using T7 and SP6 RNA polymerase, respectively, by using an *in vitro* transcription kit (MEGAscript, Invitrogen). Single-stranded sense and antisense RNA molecules were pooled together in an Eppendorf tube, and incubated (65 °C for 10 min, then 37 °C for 30 min) in a dry bath to generate dsRNA molecule of the target gene. DsRNA synthesis was confirmed by resolving a 2 μL dsRNA aliquot on 1.0% (w/v) agarose gel. Additionally, dsRNA of an unrelated gene (green fluorescent protein or GFP) was generated and included as the non-native control.

2.8. RNAi soaking of worms and behavioral assay

Approximately 500 preJ2s were rinsed with DEPC (diethyl pyrocarbonate)-treated water and soaked in soaking buffer [23]

containing 1 mg mL^{-1} target gene dsRNA in a microcentrifuge tube for 24 h in dark at room temperature. The soaking buffer contained the following constituents: "22 mM KH_2PO_4, 42.3 mM Na_2HPO_4, 85.6 mM NaCl, 1 mM $MgSO_4$, 50 mM octopamine". J2s soaked in soaking buffer containing GFP dsRNA served as the control. DsRNA uptake within the nematode body was visibly ascertained by using dsRNA molecules that were labelled with a fluorescent dye Alexa Fluor. For this, dsRNAs were custom synthesized and fused with Alexa Fluor 488 dUTP (Thermo Fisher Scientific). A fluorescence microscope (Zeiss Axiocam MRm; excitation wavelength - 488 nm; emission wavelength - 520 nm) was used to track dsRNA ingestion in nematodes.

Upon 24 h of soaking, J2s were rinsed with DEPC water several times. Total RNA was isolated from J2s followed by reverse transcription to cDNA as explained earlier. Target-specific knockdown of chemosensory genes (due to RNAi) was assessed via qPCR in a thermal cycler. qPCR reaction conditions was identical as described above.

DsRNA-treated worm behavioral assay was performed in Pluronic PF-127 gel medium in a 50 × 10 mm Petri dish. 23 g of PF-127 powder (Sigma-Aldrich) was dissolved in 80 mL of distilled water by constant stirring at 4 °C to prepare the 23% gel [24]. Root tip of 4–5 days-old germinated rice seedling was put in the middle of the plate containing 23% of PF-127 gel (Sigma). Around 25–30 J2s were inoculated via pipette at 1.5 cm behind the root tip and locomotion behavior or proprioception of J2s as crawling patterns and locomotory tracks inscribed on gel (after 1 h of inoculation) was documented under the Zeiss Axiocam MRm microscope (Carl Zeiss). Each treatment contained 3 replicates and repeated three times.

2.9. Attraction and infectivity assay

To assess the host finding ability of dsRNA-treated worms, ~ 50 J2s were inoculated via pipette at 1.5 cm behind the root tip of 4–5 days-old germinated rice seedling in a Petri plate (50 × 10 mm) containing 23% PF-127 medium. Plates were incubated in controlled and moist environment at 28 °C, 60% relative humidity. J2s attracted to the root tip were microscopically quantified at 2, 4, 6, 8, and 16 h post inoculation (hpi). To analyze the penetration ability of dsRNA-treated worms in host roots, root tips were stained with acid fuchsin [24] at 24, 48, and 72 hpi. Further, to examine the parasitic ability of dsRNA-treated worms in host roots, ~ 50 J2s were inoculated in the vicinity of rice root tip in large Petri dishes (110 × 25 mm, HIMEDIA) containing 23% PF-127 medium. Plates were incubated in a growth chamber. At 16 days post inoculation (dpi), *M. graminicola* parasitic potential was assessed via different parameters such as number of galls induced in the host root, number of egg masses (as each adult female produces its progeny in an egg mass, the count of egg mass resembles the count of successfully reproducing female), number of eggs per egg mass, and nematode multiplication factor (MF) ratio. MF ratio [(number of egg mass × number of eggs per egg mass) ÷ primary inoculation number] determines the nematode reproductive potential in a host root [25]. Each treatment constituted at least 5 replicates and repeated at least thrice.

2.10. Chemotaxis assay

The chemotactic response of dsRNA-soaked worms towards different test compounds (volatile, non-volatile and root exudates) were assessed in a 50 × 10 mm Petri dish (Sigma) containing 23% PF-127 medium [26]. 10 μL of test compounds (in different concentrations; 10^{-2} for volatiles, 200 μM for organic acids, phenolics and phytohormones, 5 μM for amino acids and carbohydrates) were pipetted in a 1.5 mm diameter hole located at 1.5 cm distance from the center of the dish. The diluent (ethanol or water, in which test compounds were dissolved) of the test compounds were pipetted at the opposite ends, which were 1.5 cm distant from the center of the plate. Upon chemical gradient establishment (took 40 min after pipetting of test compounds), ~ 100 J2s were pipetted in the center of the dish. Plates were incubated at room temperature. After 60 min of nematode inoculation, J2s accumulated towards the test compound side and diluent side were microscopically counted. The chemotaxis index (CI) was determined as the number of J2s accumulated at test compound end minus the number of J2s accumulated at diluent end divided by the cumulative counts of inoculated nematodes. CI ranged from 1.0 (perfect attraction) to −1.0 (perfect repulsion). In addition to different test compounds, root exudates (diluent was sterile water in this case) of different host plants were also used to analyze the CI of RNAi worms. Each treatment constituted at least 5 replicates and repeated at least thrice.

2.11. Statistical analysis

Initially, data of different experiments were assessed for normality via Shapiro-Wilk test. Data were either compared pairwise via *t*-test or subjected to one-way ANOVA followed by Tukey's honest significant difference (HSD) test (for multiple comparisons between treatments) in SAS v. 14.1 software.

3. Results

3.1. Molecular characterization of Mg-odr-1 and Mg-odr-3 genes from M. graminicola

By employing 5′ and 3′ RACE-PCR and primer walking, single cDNAs (RNA was extracted from the preJ2s of *M. graminicola*) containing the entire coding sequences of *Mg-odr-1* and *Mg-odr-3* were obtained, independently. NCBI Genbank accession numbers obtained for *Mg-odr-1* and *Mg-odr-3* are OQ798897 and OQ445595, respectively. The open reading frame (ORF) of *Mg-odr-1* (4869 bp) and *Mg-odr-3* (1095 bp) encode 1622 and 364 amino acids (aa), respectively. The predicted Mg-ODR-1 protein sequence corresponds to a calculated molecular mass of 184,110 Da and an isoelectric point of 8.70. The predicted Mg-ODR-3 protein sequence corresponds

to a calculated molecular mass of 41,721 Da and an isoelectric point of 5.65.

Predicted Mg-ODR-1 sequence contains a signal peptide, ligand-binding site (67–389 aa), three transmembrane motifs (136–158, 442–464 and 1541–1563 aa), extracellular protein kinase/PK (472–769 aa) and guanylyl cyclase/GCY (840–970 aa) domains, and UDP-glucosyltransferase/UDP-GT (1093–1570 aa) domain (Fig. 1A; Supplementary Fig. 1). Additionally, Mg-ODR-1 contains 9 N-glycosylated asparagine-any amino acid-serine/threonine residues and 10 O-glycosylated serine or threonine residues; four conserved cysteine residues at the intracellular domain and one each at protein kinase and guanylyl cyclase domain (Supplementary Fig. 1). Predicted Mg-ODR-3 sequence (no signal peptide) contains a transmembrane region (258–278 aa) and Gα domain (36–364 aa). Within the Gα domain, five motifs (G1-G5) are implicated in guanine nucleotide binding and hydrolysis. G1 (39–52 aa), G2 (182–190 aa) and G3 (206–215 aa) are extracellularly localized, G4 (275–282 aa) and G5 (334–339 aa) are intracellular in nature (Fig. 1B). Mg-ODR-3 contains one each of N- and O-glycosylated residues. Three conserved cysteine residues were found in Gα domain (Supplementary Fig. 2).

Pairwise sequence alignment indicated that *C. elegans* ODR-1/GCY-10 sequence was quite shorter than *M. graminicola* ODR-1 and lacked the UDP-GT domain. The ligand-binding region (amino acid sequence identity - 23.5%, similarity - 43.4%) and protein kinase domain differed considerably between these nematodes (identity - 36.3%, similarity - 58.2%), while GCY domain was quite identical (identity - 64.9%, similarity - 84%) (Fig. 1C; Supplementary Fig. 3). Conversely, *C. elegans* ODR-3/Gα sequence was quite identical to that of *M. graminicola* (overall identity - 75%, similarity - 87.6%) (Fig. 1D; Supplementary Fig. 4).

To analyze the sequence conservation of chemosensory genes in phylum Nematoda, amino acid sequences of Mg-ODR-1 and Mg-ODR-3 were used as the query to obtain the homologous/orthologous sequences from PPNs, animal-parasitic and free-living nematodes using BLASTp algorithm in WormBase Parasite as well as NCBI non-redundant database. Highly similar ODR-1 (Percent identity: 42–89%, Query coverage: 51–100%, Expect value: 0.0) and ODR-3 (Percent identity: 57–95%, Query coverage: 66–100%, Expect value: 0.0) sequences were included in phylogeny studies (all the obtained homologues/orthologues were separately annotated to detect expected functional domains/motifs). The phylogenetic tree was rooted against the corresponding ODR orthologues from *Drosophila melanogaster* as the outgroup. Expectedly, ODR-1 of *M. gramincola* clustered with that of other PPNs (belong to the clade 10

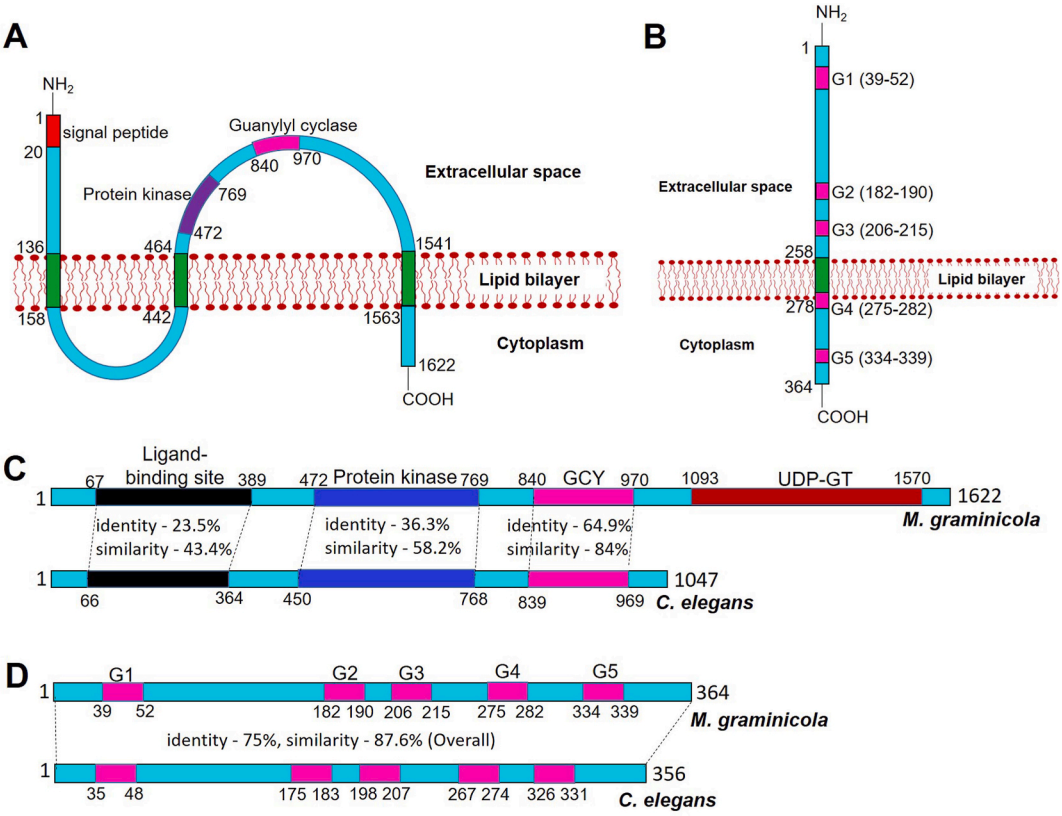

Fig. 1. The predicted secondary structures of Mg-ODR-1 and Mg-ODR-3 protein. **(A)** Mg-ODR-1 contains amino-terminal signal peptide, three transmembrane motifs (136–158, 442–464 and 1541–1563 aa), extracellular protein kinase (472–769 aa) and guanylyl cyclase (840–970 aa) domains, and intracellular carboxyl termini. **(B)** Mg-ODR-3 contains a transmembrane motif (258–278 aa) and Gα domain (36–364 aa) characteristic of three extracellular motifs G1 (39–52 aa), G2 (182–190 aa), G3 (206–215 aa), and two intracellular motifs G4 (275–282 aa) and G5 (334–339 aa). **(C)** Schematic alignment of ODR-1/GCY-10 sequence of *C. elegans* (NCBI accession: NP_001362115) with that of *M. graminicola*. *C. elegans* ODR-1 lacks UDP-GT domain. Percent sequence identity and similarity between different domains are shown. **(D)** Schematic alignment of ODR-3/Gα sequence of *C. elegans* (NCBI accession: NP_506290) with that of *M. graminicola*. Numbers indicate amino acid sequence coordinates.

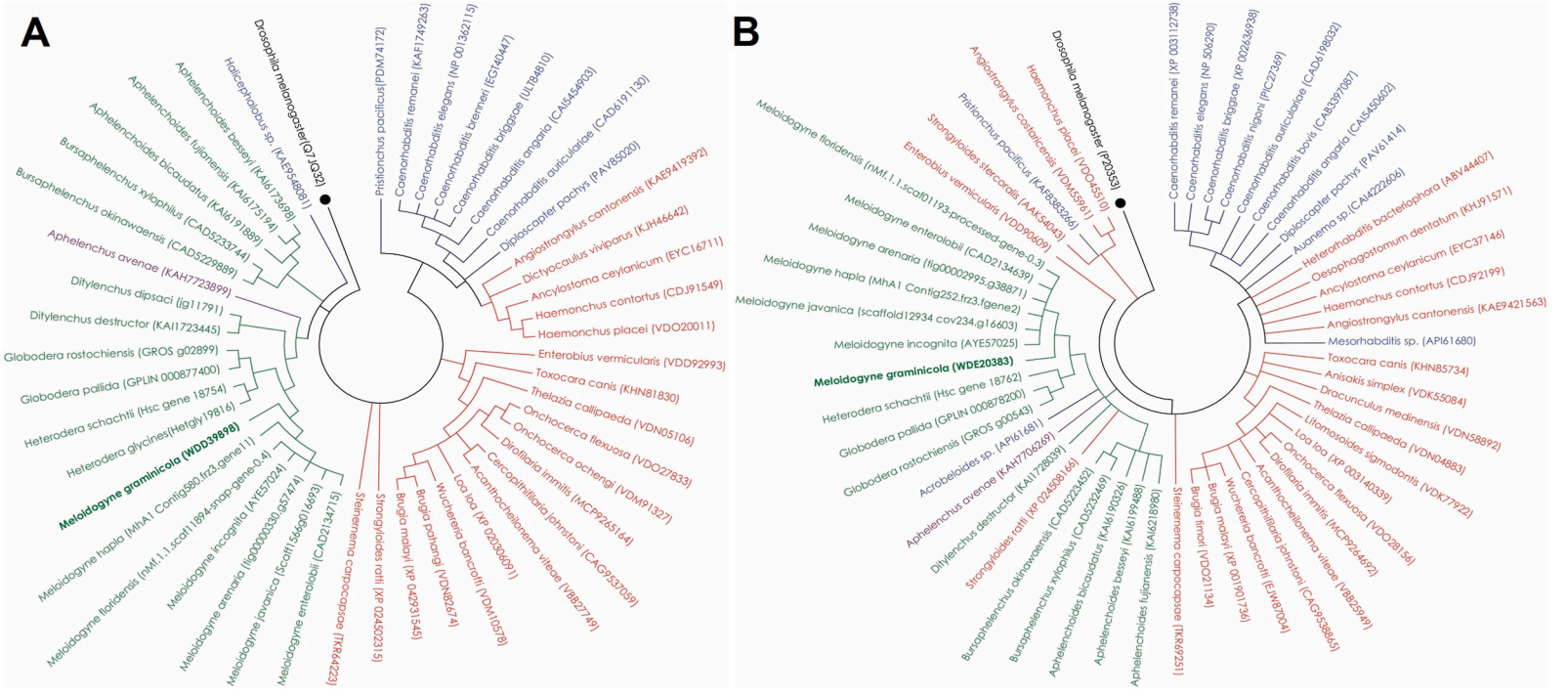

Fig. 2. Evolutionary relationship of Mg-ODR-1 **(A)** and Mg-ODR-3 **(B)** protein from *M. graminicola* with their corresponding homologues from other nematode species. The phylogenetic tree was constructed in MEGA6 software using Maximum Likelihood method based on Tamura 3-parameter model. Bootstrap consensus was inferred from 1000 replicates and branches corresponding to <70% replicates were collapsed. NCBI accession numbers and WormBook Parasite gene identifiers of different entries are provided in parentheses. All gaps and missing data positions were eliminated after sequence alignment. *Drosophila melanogaster* sequence for the corresponding protein was used as the out-group (marked with ●). Entries in green, red, blue and purple correspond to the plant-parasitic, animal-parasitic, free-living and fungivorous nematodes, respectively.

and 12 of phylum Nematoda) that branched away from ODR-1 sequences of animal-parasitic (including insect-parasitic) and free-living bacterivorous nematodes. However, PPN branch contained an entry each of fungivorous (*Aphelenchus avenae*, clade 12) and bacterivorous (*Halicephalobus* sp., clade 11) nematodes. Intriguingly, PPN group contained different subgroups for *Meloidogyne* spp., *Heterodera/Globodera* spp., *Ditylenchus* spp. (clade 12), *Bursaphelenchus* spp. and *Aphelenchoides* spp. (clade 10), suggesting ODR-1 sequence divergence between PPN groups of different feeding habits (Fig. 2A). A similar trend was observed for ODR-3 sequences; PPN branch contained entries from *A. avenae*, bacterivorous *Acrobeloides* sp. (clade 11) and animal-parasitic *Strongyloides ratti* (clade 10). Insect-parasitic *Steinernema carpocapsae* (clade 10) branched farther from *Heterorhabditis bacteriophora* (clade 9) (Fig. 2B). Nevertheless, a high-degree of pan-phylum conservation of *M. graminicola* ODR1/3 (encompassing clades 2, 8, 9, 10, 11 and 12; Supplementary Fig. 5) is evident from our analysis because both ODR-1 and ODR-3 homologues were represented in ~54 species of phylum Nematoda (as per the accessible sequences in multiple databases).

The motif characteristics (in terms of motif numbers and location) of Mg-ODR-1 and Mg-ODR-3 were conserved across the different nematode species of phylum Nematoda. For Mg-ODR-1, although PK and GCY motifs were conserved in majority of the species but they lacked UDP-GT motif. A reduced complement of Mg-ODR-1 protein was observed in *Meloidogyne floridensis* (lacked PK motif), *Wuchereria bancrofti*, *Onchocerca ochengi* (lacked GCY motif), *Parelaphostrongylus tenuis*, *Caenorhabditis nigoni*, *Auanema* sp. and *Trichuris suis* (lacked PK and GCY motifs) (Supplementary Fig. 6). This maybe because a number of corresponding cDNA sequences of those entries are mere partial, not full-length one. For Mg-ODR-3, all the five motifs (G1 to G5) were located in majority of the species except *Meloidogyne javanica*, *Mesorhabditis* sp., *Anisakis simplex*, *Oesophagostomum dentatum* and *Ancylostoma ceylanicum* (Supplementary Fig. 7).

3.2. Stage-specific expression profiles of *Mg-odr-1* and *Mg-odr-3* in *M. graminicola*

To investigate the differential transcript abundance of *Mg-odr-1* and *Mg-odr-3* genes across the developmental stages of *M. graminicola*, RT-qPCR was carried out. Compared to the expression levels in post egg laying adult females (fold change value was set

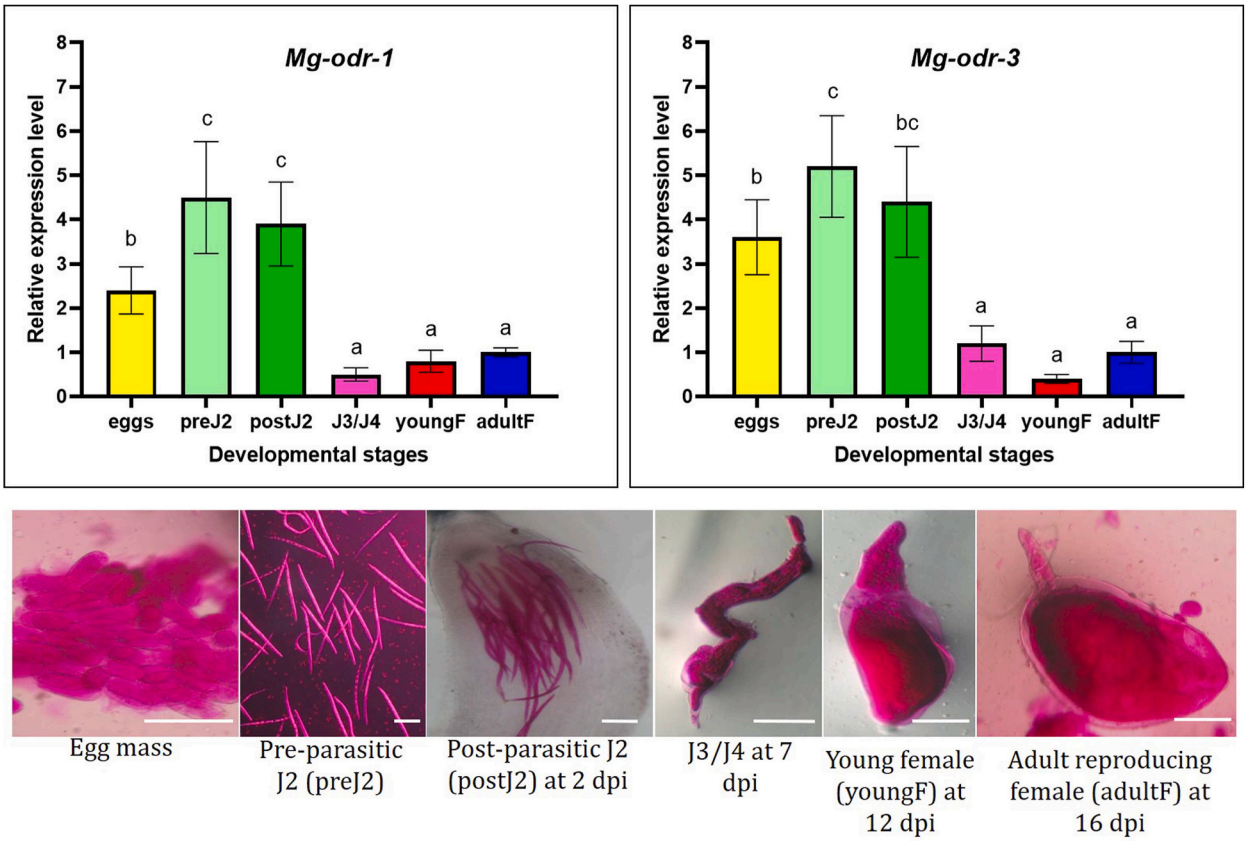

Fig. 3. Relative expression level of *Mg-odr-1* and *Mg-odr*-3 mRNAs in different life stages of *M. graminicola*. Fold change in target gene expression was set as 1 in adult female, and statistically compared with expression in other developmental stages including egg, pre- and post-parasitic J2, J3/J4, young and adult female. Each bar represents mean fold change value of qPCR runs in three biological and technical replicates ± standard errors. Bars with different letters indicate significant difference according to the Tukey's HSD test, $P < 0.01$. Gene expression was normalized using two housekeeping genes of *M. graminicola* (actin and *18S rRNA*). Bottom panel represents different life stages stained with acid fuchsin. Scale bar = 100 μm.

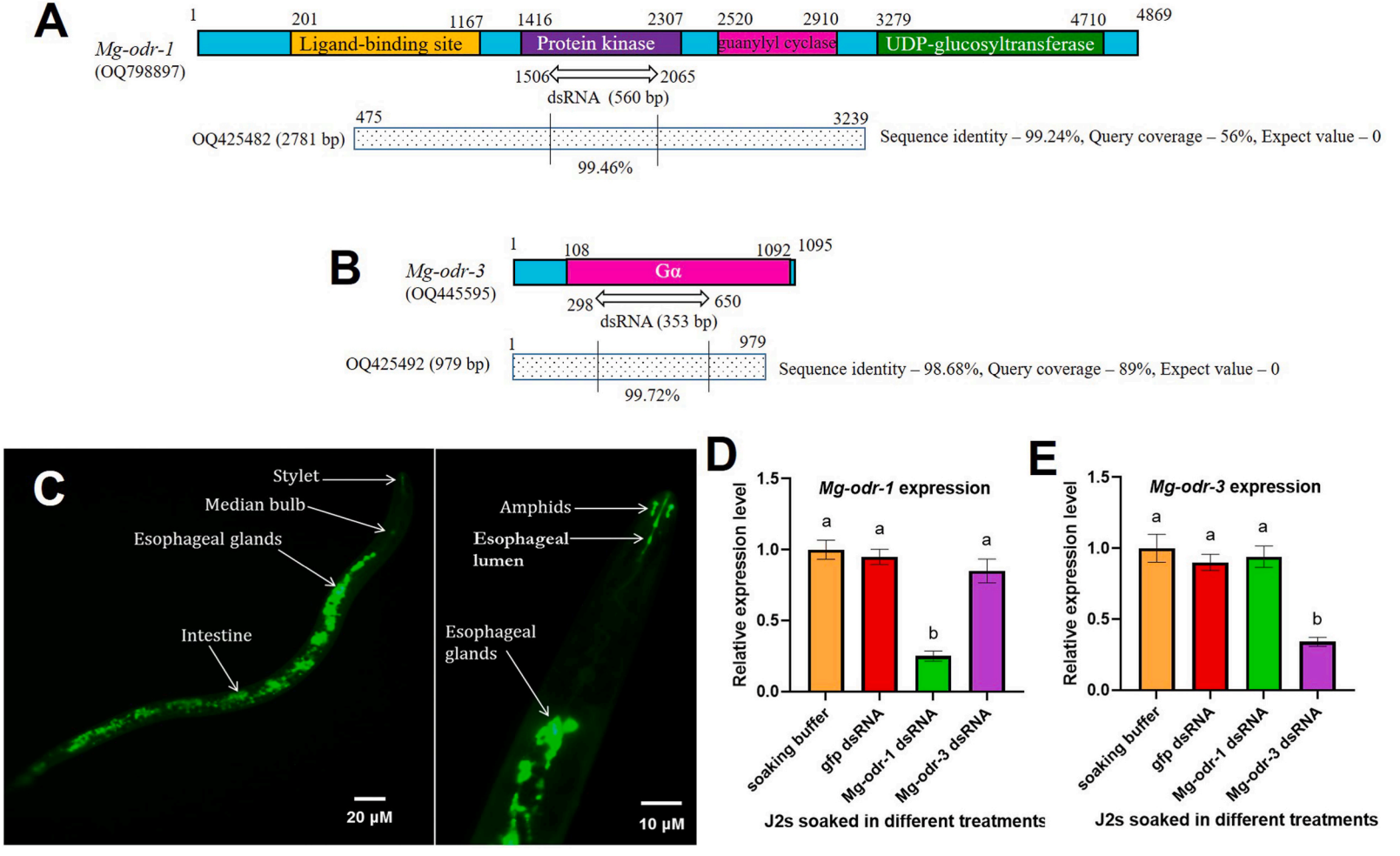

Fig. 4. RNAi-induced silencing of chemosensory genes in *M. graminicola* pre-parasitic J2. Illustration of *Mg-odr-1* **(A)** and *Mg-odr-3* **(B)** open reading frames showing conserved domains (solid colored boxes), targeted sites for dsRNA synthesis (indicated by two-headed arrows) and homologous *M. graminicola* transcripts obtained from NCBI non-redundant database. Numbers represent the sequence coordinates. Genbank accession numbers are provided in parentheses. **(C)** A representative fluorescent photomicrograph demonstrates the uptake of Alexa Fluor-labelled *Mg-odr-1* dsRNA in different body parts of *M. graminicola* J2 at 24 h post soaking. Target-specific downregulation of *Mg-odr-1* **(D)** and *Mg-odr-3* **(E)** mRNAs in J2s treated with corresponding dsRNAs at 24 h post soaking. Nematodes treated with *gfp* dsRNA and soaking buffer were used as the non-native and negative control, respectively. *M. graminicola* actin and *18S rRNA* genes were used to normalize the fold change in expression data. Each bar represents mean fold change value of qPCR runs in three biological and technical replicates ± standard errors. Fold change in target gene expression was set as 1 in soaking buffer-treated worms, and statistically compared with other treatments. Bars with different letters indicate significant difference according to the Tukey's HSD test, $P < 0.01$.

as 1 as the reference), both *Mg-odr-1* and *Mg-odr-3* mRNAs were significantly ($P < 0.01$) upregulated in eggs, pre- and post-parasitic J2s (highest expression documented in pre and postJ2s) and were unaltered ($P > 0.01$) in J3/J4 stages and young/immature female stages (Fig. 3). Our results suggested that *M. graminicola* chemotaxis-related genes are predominantly transcribed in early life stages including eggs and J2s.

3.3. RNAi-induced knockdown of chemotaxis-related genes caused aberrant behavioral phenotypes in M. graminicola

Target dsRNA molecules were designed from the open reading frames (ORFs) of *Mg-odr-1* (Fig. 4A) and *Mg-odr-3* (Fig. 4B) by employing the following important criterion: (i) targeted region should preferentially be 400–500 bp long for efficient processing of dsRNA molecules by Dicer enzymes, (ii) selected sites must predict maximum siRNA formation probabilities compared to the non-targeted sites of the identical gene. Next, when dsRNA sequences corresponding to *Mg-odr-1* (560 bp) and *Mg-odr-3* (353 bp) genes were aligned together, a highly discontinuous sequence identity was documented (Supplementary Fig. 8). Further, selected dsRNA

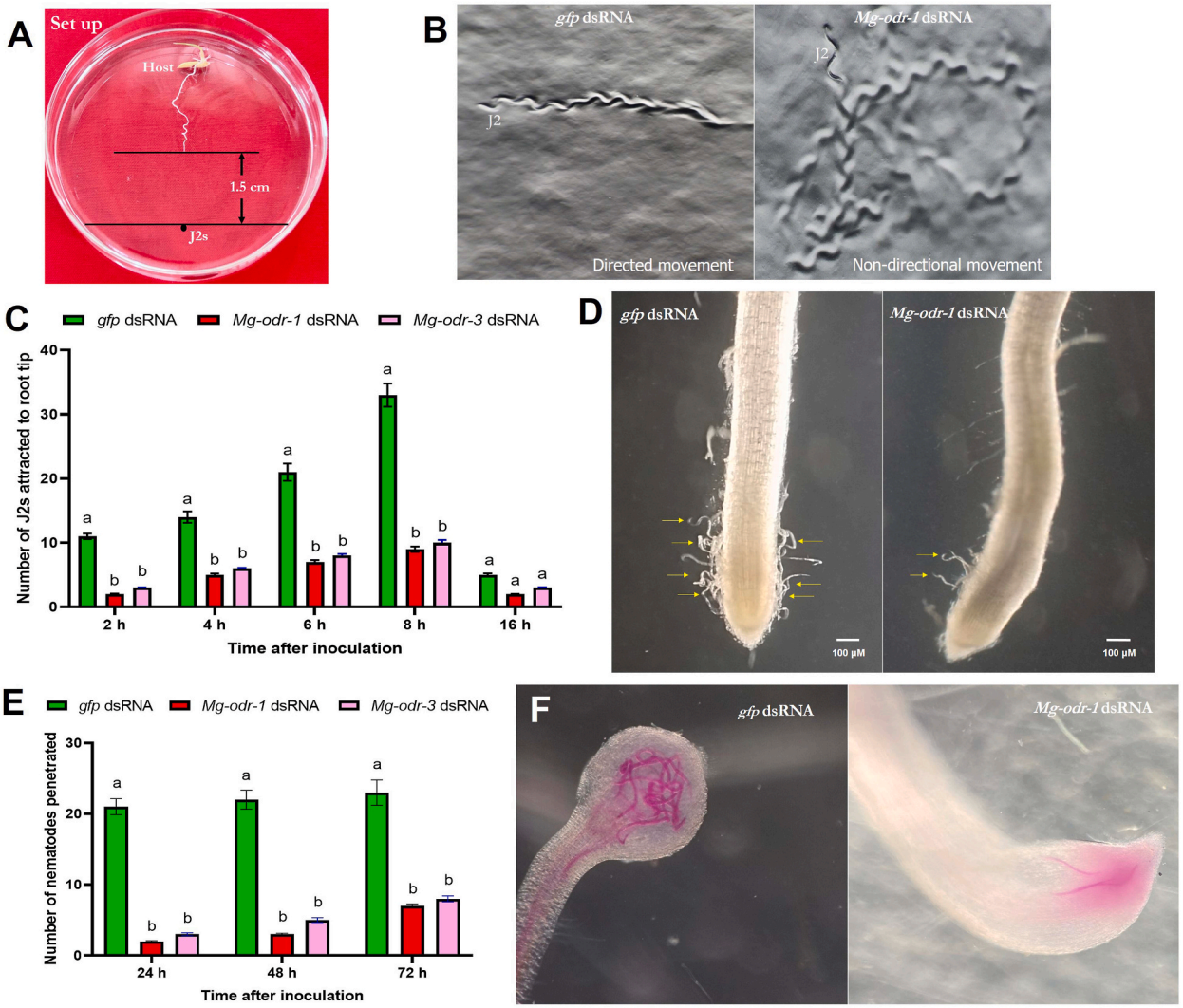

Fig. 5. RNAi-induced silencing of chemosensory genes altered behavioral phenotypes of *M. graminicola*. **(A)** Set up of the behavioral assay is described. Root tip of rice seedling was kept at the center of the Petri dish (50 × 10 mm) containing Pluronic gel medium and J2s were inoculated at 1.5 cm posterior to the root tip. **(B)** Tracking pattern indicated non-directional locomotion of *Mg-odr-1* dsRNA-treated J2s compared to the normal sinusoidal locomotion of control J2s. Attraction **(C)** and penetration **(E)** of *Mg-odr-1* and *Mg-odr-3* dsRNA-treated J2s to rice root at different time points. J2s treated with *gfp* dsRNA served as the control. Each bar represents mean number of nematodes per root system in three biological and five technical replicates ± standard errors. Bars with different letters indicate significant difference according to the Tukey's HSD test, $P < 0.01$. **(D)** Photomicrographs depict considerably lower host attraction potential of *Mg-odr-1* silenced worms than control J2s at 8 h after inoculation. Yellow arrowheads indicate J2s latching on to the rice root tip. **(F)** Photomicrographs depict considerably lower host penetration ability of *Mg-odr-1* silenced worms than control J2s at 48 h after inoculation. Root segments were stained with acid fuchsin.

sequences were queried against the siRNA database of multiple organisms in DsCheck (http://dscheck.rnai.jp/) server to examine the RNAi-induced probable off-target effects. SiRNAs processed from *Mg-odr-1* and *Mg-odr-3* dsRNA did not show considerable matches with siRNA databases of *Drosophila melanogaster*, *Rattus norvegicus*, *Oryza sativa* and *Arabidopsis thaliana*. Nevertheless, *Mg-odr-1* and *Mg-odr-3* siRNAs did show homology to GCY and Gα domains of *C. elegans*.

J2s were soaked in *in vitro* synthesized dsRNA solutions for 24 h. Fluorescence microscopy examinations showed that nematodes can successfully uptake the Alexa Fluor-labelled dsRNAs (Fig. 4C). Compared to soaking buffer-treated worms, a 75 and 66 % repression ($P < 0.01$) of *Mg-odr-1* and *Mg-odr-3* transcripts (determined by qPCR analysis) were documented in *Mg-odr-1* and *Mg-odr-3* dsRNA-treated J2s, respectively (Fig. 4D and E). *Mg-odr-1* and *Mg-odr-3* expressions were alike ($P > 0.01$) of soaking buffer-treated worms in *gfp* dsRNA-soaked J2s (Fig. 4D and E), indicating that *gfp* dsRNA itself did not affect the target olfactory gene expression. Expression of *Mg-odr-1* was not attenuated ($P > 0.01$) in *Mg-odr-3* dsRNA-soaked worms and vice versa (Fig. 4D and E). This establishes the RNAi-induced target-specific knockdown of chemosensory genes in our study. However, *Mg-odr-1* and *Mg-odr-3* share a sequence identity of 99.24 and 98.68% with the homologous transcripts OQ425482 and OQ425492, respectively (Fig. 4A). In addition, only 2–3 nucleotides were varying between gene and homologous transcript in the dsRNA target regions, suggesting that RNAi of *Mg-odr-1* and *Mg-odr*-3 might have silenced their other allelic variants in *M. graminicola*. However, this hypothesis could not be proven, because suitable primers, which would demarcate these highly homologous transcripts, could not be designed.

Behavior phenotypes of RNAi worms (24 h after dsRNA treatment) were examined by multiple assays. Firstly, dsRNA-treated J2s were inoculated at 1.5 cm distance from the rice root tip in Pluronic gel medium and nematode movement patterns towards root were analyzed (Fig. 5A). *Mg-odr-1* dsRNA-treated J2s exhibited non-directional (dwelling behavior) locomotion compared to the directional movement (sinusoidal proprioception) in dsGFP control worms (Fig. 5B), suggesting that RNAi of chemotaxis-related genes can affect *M. graminicola* host seeking potential. A similar tracking pattern was observed in *Mg-odr-3* dsRNA-treated J2s (data not shown).

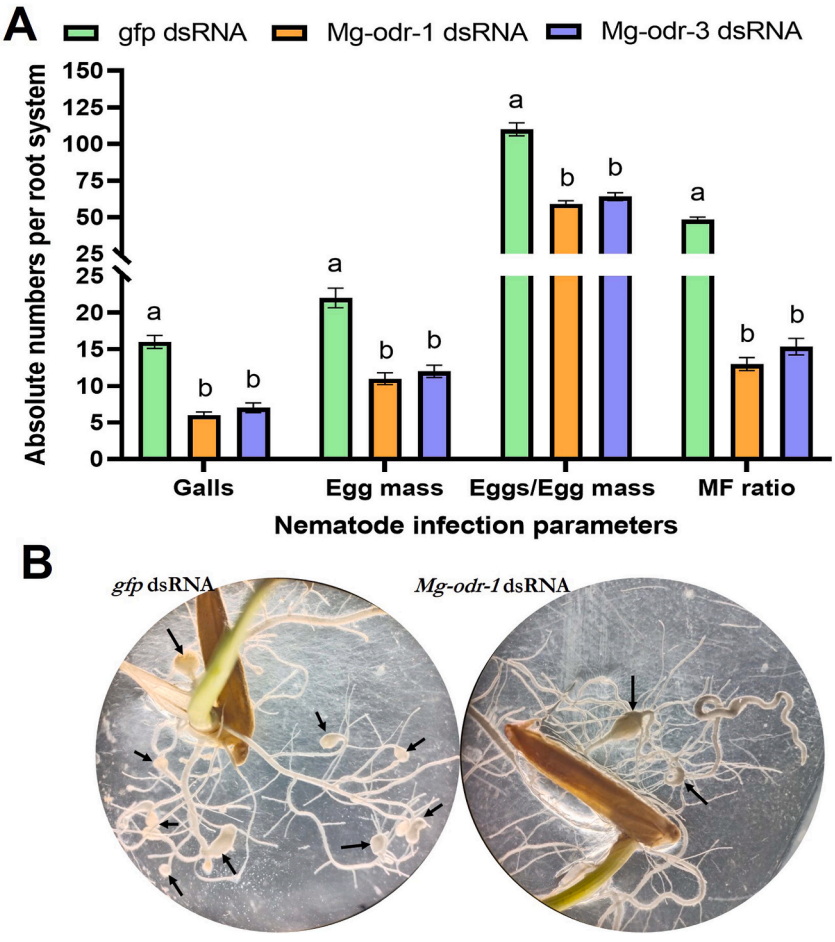

Fig. 6. RNAi-induced silencing of chemosensory genes attenuated parasitic potential of *M. graminicola* in rice root. **(A)** Comparatively lower number of galls, egg masses, eggs per egg mass and multiplication factor (MF) ratio were documented in rice roots infected with *Mg-odr-1* and *Mg-odr-3* silenced worms than the roots infected with control J2s. Each bar represents mean numbers (of different infection parameters) per root system in three biological and five technical replicates ± standard errors. Bars with different letters indicate significant difference according to the Tukey's HSD test, $P < 0.01$. **(B)** Photographs depict comparatively lower galling intensity in host roots infected with *Mg-odr-1* silenced worms than the roots infected with control worms. Black arrowheads indicate root galls.

Consequently, both *Mg-odr-1* and *Mg-odr-3* dsRNA-soaked J2s were attracted in considerably lower ($P < 0.01$) numbers to rice root tips compared to the dsGFP worms (Fig. 5C and D). RNAi-induced negative host attraction behavior of *M. graminicola* J2 was correlated with the reduced host invasion ability because both *Mg-odr-1* and *Mg-odr-3* dsRNA-treated J2s penetrated rice roots in substantially lower ($P < 0.01$) numbers compared to the dsGFP worms (Fig. 5E and F).

RNAi-induced aberrant behavior of *M. graminicola* J2s ultimately affected their parasitic success in rice. Number of galls, egg

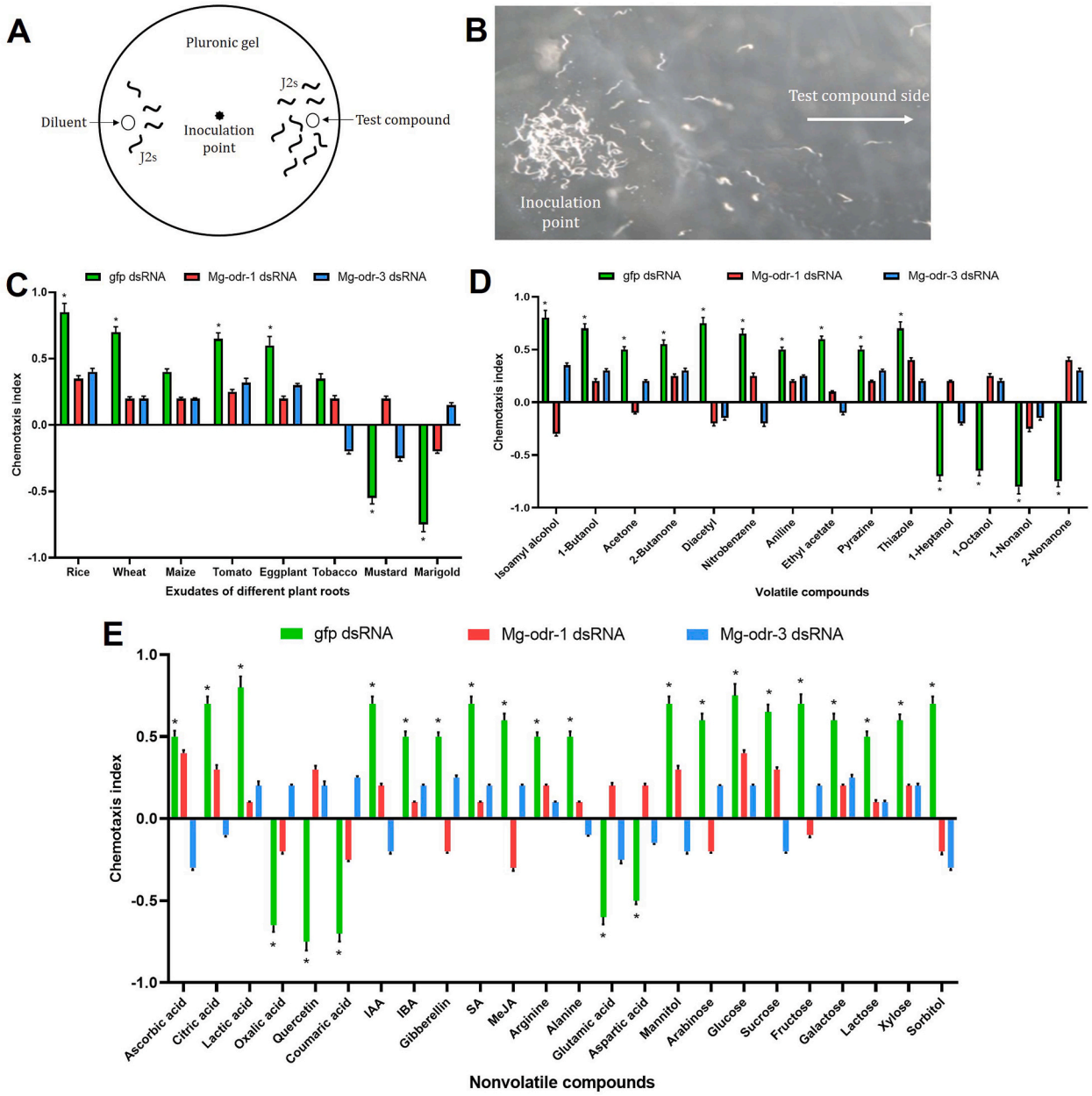

Fig. 7. RNAi-induced silencing of chemosensory genes affected *M. graminicola* chemotaxis to volatile and non-volatile compounds. **(A)** The *in vitro* assay system used is schematically represented. J2s inoculated at the center of the Petri dish (50 × 10 mm) containing Pluronic gel medium. Inoculation point was 1.5 cm equidistant from test compound and diluent (in which compounds were diluted) side. **(B)** Photomicrograph (taken at 20 min after nematode inoculation) shows the selective dispersion of *gfp* dsRNA-treated J2s towards test compound side. Comparative chemotaxis responses of *gfp* dsRNA-treated worms and *Mg-odr*-1/Mg-*odr-3* silenced worms towards different host root exudates **(C)**, volatile compounds **(D)** and nonvolatile compounds **(E)**. Chemotaxis index (CI) values vary from −1.0 to +1.0. Positive and negative values indicate attraction and repulsion, respectively. Each bar represents mean CI value in three biological and technical replicates ± standard errors. Asterisks are indicative of significant difference ($P < 0.01$, paired *t*-test) in CI values of J2s towards test compounds compared to the CI values of J2s towards water (as negative control). 10 μL of test compound was tested against ~ 100 J2s.

masses, eggs per egg mass and nematode multiplication factor (MF) ratio per root system were significantly reduced in plants infected by *Mg-odr-1* and *Mg-odr-3* dsRNA-soaked J2s compared to the plants infected by dsGFP J2s (Fig. 6A and B).

3.4. RNAi-induced knockdown of chemosensory genes caused perturbed chemotaxis in M. graminicola

To examine whether RNAi-induced downregulation of *Mg-odr-1* and *Mg-odr-3* caused aberrant chemotactic behavior in *M. graminicola*, an *in vitro* chemotaxis assay was performed against a number a test compounds in a Petri plate that contained the Pluronic gel medium (Fig. 7A and B). Chemical gradients are established within a very short time (~ 40 min) in this assay system [26]. More details about chemical gradient establishment in this assay system are provided in Supplementary Fig. 9. Initially, root diffusates of different host plants were used as the test compounds. Control J2s were significantly ($P < 0.01$) attracted to the exudates of rice, wheat, tomato and eggplant and significantly ($P < 0.01$) repelled by the diffusates of mustard and marigold. Conversely, dsRNA-soaked worms did not exhibit substantial ($P > 0.01$) attraction or repulsion response towards either of these diffusates (Fig. 7C). However, chemotaxis index (CI) did not change considerably ($P > 0.01$) in control or dsRNA-treated J2s while exposed to the exudates of maize and tobacco (Fig. 7C).

Next, RNAi-induced chemotaxis defects in *M. graminicola* was assessed against a number of volatile compounds. Prior to that, the optimum concentration of volatiles were determined by exposing the wild-type J2s to these compounds in neat concentration and serial dilutions (10°, 10^{-1}, 10^{-2}, 10^{-3}, 10^{-4} and 10^{-5}). Autoclaved ethanol @ 0.05% v/v was employed as the diluent. Majority of the compounds at higher concentrations (10°, 10^{-1}) caused lethal effect on nematodes and worms remained unresponsive towards lower concentrations (10^{-3}, 10^{-4}, 10^{-5}). Nematode chemotaxis behavior could be properly documented at 1% dose of the volatiles (10^{-2} concentration). Therefore, 10^{-2} concentration was used to assess the CI of RNAi worms. Control worms showed significant ($P < 0.01$) attraction towards 1-butanol, 2-butanone, isoamyl alcohol, acetone, nitrobenzene, diacetyl, aniline, pyrazine, ethyl acetate and thiazole, and showed significant ($P < 0.01$) repulsion towards 1-nonanol, 2-nonanone, 1-octanol and 1-heptanol (Fig. 7D). On the contrary, chemotactic behavior of *Mg-odr*-1/Mg-*odr-3* dsRNA-soaked J2s was not significantly ($P > 0.01$) altered when exposed to these selective volatiles (Fig. 7D).

Chemotaxis response of RNAi worms was also assessed against nonvolatile compounds such as organic acids (ascorbic, citric, lactic and oxalic acids), phenolics (quercetin and coumaric acid), phytohormones (gibberellin, indole-3-acetic acid or IAA, salicylic acid or SA, indole-3-butyric acid or IBA and methyl jasmonate or MeJA), amino acids (glutamic acid, arginine, aspartic acid and alanine) and carbohydrates (arabinose, mannitol, sorbitol, xylose, lactose, glucose, galactose, sucrose and fructose). As determined for volatiles, optimum concentrations of these nonvolatile compounds were determined after an intensive *in vitro* screening assays with wild-type worms. Finally, RNAi worms were exposed to 200 μM dose of organic acids, phenolics and phytohormones, and 5 mM dose of amino acids and carbohydrates. Control worms exhibited attractive behavior to citric acid, ascorbic acid, lactic acid, gibberellin, indole acetic acid, indole butyric acid, salicylic acid, methyl jasmonate, alanine, arginine, arabinose, mannitol, sorbitol, xylose, lactose, glucose, galactose, fructose and sucrose, and aversive behavior to coumaric acid, quercetin, aspartic acid, glutamic acid and oxalic acid (Fig. 7E). By contrast, CI of *Mg-odr*-1/Mg-*odr-3* dsRNA-soaked J2s was unaltered ($P > 0.01$) upon exposure to different candidate nonvolatile compounds (Fig. 7E).

4. Discussion

PPN chemoreception is an important sensory modality to find its suitable hosts. Extensive forward genetics screening in model nematode *C. elegans* has shown that sensory odorant receptors such as few GPCRs in conjunction with ligand-dependent receptors such as GCYs mediate the chemotaxis response. More specifically, GPCRs regulate cGMP production via GCY (ODR1/DAF11) to open cyclic nucleotide-gated or CNG (TAX2/TAX4) channel [15,27]. Additionally, G proteins activate its Gα (ODR3) subunit, downstream to which transient receptor potential vanilloid or TRPV (OSM9/OCR2) channel is opened and transmembrane Ca^{2+} influx occurs [28]. Opening of CNG and TRPV channels causes behavioral changes in nematode chemotaxis [15,29]. Only a few *C. elegans* chemosensory gene complements have been identified and functionally validated in PPNs including *M. incognita* and *Heterodera glycines* [16,30,31]. Present study advances that knowledge by characterizing two chemotaxis-related genes from the rice root-knot nematode *M. graminicola*.

Current study reports the full-length cDNA sequences of *Mg-odr-1* and *Mg-odr-3*. Mg-ODR-1 and Mg-ODR-3 proteins contain the typical GCY and Gα domains, respectively. Both Mg-ODR-1 and Mg-ODR-3 are transmembrane proteins that contain conserved cysteine residues and a number of N- glycosylated and O-glycosylated residues. Conserved cysteine residues may constitute disulfide bonds to provide the conformational change in receptor proteins for ligand-binding [32]. Glycoproteins including N-glycans and O-glycans undergo covalent binding with proteins and lipids for forming glycoconjugates, which aid in tethering to the cell membrane lipids. A number of receptor proteins contain N- and O-glycosylated residues [33,34]. In *C. elegans*, the primary role of GCY receptors is to modulate and transduce the chemosensory signals by dimerizing its half-cyclase domains. This dimerization is regulated by ligand binding to its receptor domain. Additionally, its protein kinase domain aids in protein phosphorylation [35,36]. The extracellular ligand-binding domain showed extensive heterogeneity across the members of GCY family in *C. elegans*. This maybe because *C. elegans* has experienced evolutionary pressures to diversify its ligand-binding domain in order to perceive and respond to a wider-spectrum of ligands via its GCY receptors, and eventually this metazoan evolved to respond to chemical cues, which otherwise do not interact with classical GPCRs [36–38]. Notably, in our analysis, the ligand-binding domain of ODR-1 substantially differed between *C. elegans* and *M. graminicola*. Intriguingly, in our *M. graminicola* ODR-1 sequence we encountered an additional UDP-GT domain, which was absent in corresponding *C. elegans* sequence. In animals and insects, UDP-GT has been implicated in olfaction process where it specifically acts

as an odorant degrading enzyme that detoxifies the stimulus molecule (to prevent receptor saturation) in concurrence with the odor detection by GCYs [39–41]. The ODR-3 sequence was quite identical between *C. elegans* and *M. graminicola* in our analysis. Taken together, it is speculated that both Mg-ODR-1 and Mg-ODR-3 may function as receptor proteins during the complex chemotaxis mechanism in *M. graminicola*.

Phylogenetic analyses indicated that both Mg-ODR-1 and Mg-ODR-3 are evolutionarily more conserved in PPN branch, and are quite distant from their homologous sequences in animal-parasitic and free-living worms. This maybe because PPNs have independently evolved within the phylum Nematoda for at least three times [42]. However, ODR sequence divergence was evident between cyst (*Heterodera* spp., *Globodera* spp.) and root-knot (*Meloidogyne* spp.) nematodes. This finding maybe attributed to the differential evolution of chemotaxis-related genes in cyst and root-knot nematodes owing to their differential host preferences. This information would be advantageous while designing novel nematicide or drug molecules (that target nematode chemosensory function), which might show broad-spectrum efficacy against root-knot nematodes without affecting the off-target nematodes. Intriguingly, PPN branches for both Mg-ODR-1 and Mg-ODR-3 contained an entry of fungivorous nematode *Aphelenchus avenae* (clade 12 of phylum Nematoda), indicating *A. avenae* to be the possible point of radiation of *odr-1* and *odr-3* genes in plant-parasitic clades. Based on phylogeny of small-subunit ribosomal DNA sequences, Holterman et al. [43] concluded that PPNs arose from their fungivorous ancestors.

Developmental stage-dependent gene expression data showed that *Mg-odr-1* and *Mg-odr-3* are specifically transcribed in eggs, preparasitic J2 and post-parasitic J2 stages, exemplifying the putative role of these genes in early parasitic stages of *M. graminicola* probably aiding in nematode host location and finding of a suitable feeding cell inside the host tissue. The association of these genes in nematode host finding was confirmed by RNAi-based functional validation strategy. Firstly, any abnormality in behavioral pattern was validaed in olfactory gene-silenced nematodes. RNAi nematodes exhibited non-directional locomotion towards rice root tip in Pluronic gel medium compared to the directional movement of control nematodes. Accordingly, RNAi nematodes were attracted to the rice root tip in lower numbers compared to the control nematodes at 2 h, 4 h, 6 h and 8 h after inoculation. However, at 16 h after inoculation, attraction data did not differ significantly between RNAi and control worms, possibly because of the transient nature of RNAi effect [44,45] or most of the attracted nematodes had penetrated the rice root. Roots stained with acid fuchsin dye at 24, 48 and 72 h showed that RNAi worms had penetrated the host root in lower numbers compared to the control worms. Notably, *Mg-odr-1* and *Mg-odr-3* silenced *M. graminicola* had reduced parasitic success in rice root as estimated by different infection parameters including gall number, egg mass formation, eggs produced per egg mass and MF ratio (determines nematode reproductive potential in subsequent generation in a host crop) data. This maybe because of the indirect consequences of attenuated host finding ability of RNAi worms.

Host root exudates contain various bioactive compounds that selectively modulate PPN chemotactic response in terms of attraction, repulsion or motility inhibition [8,46]. Root exudates contain a wide spectrum of compounds including nonvolatiles such as sugars, organic acids, amino acids, fatty acids, growth hormones, sterols, flavonoids etc., and volatiles such as alcohols, glucosinolates, isothiocyanates, alkyl sulfides, CO_2, HCO_3, inorganic ions etc. [47]. Earlier findings indicated that *C. elegans* selectively chemo-orientate towards different volatile compounds including organic acids, alcohols, amine components, esters, aromatic molecules, ketone components and heterocyclic molecules using its ODR receptor proteins [36,48,49]. Additionally, our earlier study demonstrated that the PPN *M. incognita* can differentially chemotax to different volatile and nonvolatile compounds, and loss of chemosensory gene activity selectively alters the worm chemotaxis behavior [16]. In this direction, we first assessed the chemotactic response of *M. graminicola* wild-type J2s towards different test compounds (including root exudates, volatiles and nonvolatiles) followed by assessing the chemotactic potential of RNAi J2s towards the identical compounds.

Notably, control (*gfp* dsRNA-treated) J2s were attracted to the root diffusates of rice, wheat, tomato and eggplant, and repelled by the diffusates of mustard and marigold. This selective chemotactic behavior was variably altered in RNAi (*Mg-odr*-1/Mg-*odr-3* dsRNA-treated) J2s. In parallel, RNAi J2s were not attracted to volatiles such as 1-butanol, 2-butanone, isoamyl alcohol, diacetyl, nitrobenzene, acetone, ethyl acetate, thiazole, pyrazine and aniline, which were attractive to the wild-type worms. Similarly, RNAi J2s were not repelled to 1-octanol, 2-nonanone, 1-nonanol and 1-heptanol, which were repellent for the wild-type worms. Additionally, RNAi J2s were not attracted to nonvolatiles such as ascorbic acid, citric acid, lactic acid, indole acetic acid, indole butyric acid, salicylic acid, methyl jasmonate, gibberellin, alanine, arginine, arabinose, mannitol, xylose, sucrose, lactose, galactose, sorbitol, fructose and glucose, which were found to be attractant for wild-type J2s. Similarly, RNAi J2s did not show aversive behavior to coumaric acid, quercetin, aspartic acid, glutamic acid and oxalic acid, which were otherwise repellent to wild-type J2s. Collectively, all these results suggest that RNAi-induced targeted downregulation of *Mg-odr-1* and *Mg-odr-3* noticeably perturbed the *M. graminicola* chemotaxis behavior, establishing the crucial role of *Mg-odr-1* and *Mg-odr-3* in *Meloidogyne graminicola* olfaction and nociception mechanism. The adaptive olfactory responses (ability to selectively discriminate different compounds) of PPNs such as *M. incognita* and *Globodera pallida* towards different phytochemicals such as sugars, amino acids, hormones, phenolics and organic acids have been described in various studies [50–53].

In conclusion, current study demonstrates the specific role of *Mg-odr-1* and *Mg-odr-3* in *Meloidogyne graminicola* chemotaxis and host finding mechanism. The chemosensory mechanism of PPNs are associated with diverse biological processes including locomotion, host finding, host invasion and initiation of feeding sites in the host tissue. Presently, variability in PPN sensory perception to different chemical cues has been investigated, however, the causal molecular mechanism behind the typical chemosensory response is underexplored. Further research would be necessary in this direction to unravel the PPN-specific chemosensory signal transduction pathway. Identification of molecular chokepoints (that lead to aberrant PPN behavior) can result in selection of precise targets for novel nematicide development or *in planta* RNAi screens.

Data availability statement

Data are included in the article and supplementary figures and tables. NCBI Genbank accession numbers for *Mg-odr-1* and *Mg-odr-3* genes are OQ798897 and OQ445595, respectively. Additional data will be made available upon request.

CRediT authorship contribution statement

Tushar K. Dutta: Writing – review & editing, Writing – original draft, Supervision, Methodology, Investigation, Formal analysis, Conceptualization. **Voodikala S. Akhil:** Methodology, Investigation. **Artha Kundu:** Methodology, Investigation. **Manoranjan Dash:** Methodology, Investigation. **Victor Phani:** Formal analysis, Data curation. **Anil Sirohi:** Supervision, Resources. **Vishal S. Somvanshi:** Supervision, Resources.

Declaration of competing interest

The authors declare that they have no known competing financial interests or personal relationships that could have appeared to influence the work reported in this paper.

Acknowledgements

We sincerely thank Head of the Division, Nematology, Indian Agricultural Research Institute and Joint Director (research) and Director, Indian Agricultural Research Institute for supporting us with institute funding to perform the experiments.

Appendix A. Supplementary data

Supplementary data to this article can be found online at https://doi.org/10.1016/j.heliyon.2024.e26384.

References

[1] N. Hamada, H.Z. Yimer, V.M. Williamson, S. Siddique, Chemical hide and seek: nematode's journey to its plant host, Mol. Plant 13 (2020) 541–543.
[2] V.S. Mattos, K. Mulet, J.E. Cares, C.B. Gomes, D. Fernandez, M.F. Grossi-de-Sá, R.M.D.G. Carneiro, P. Castagnone-Sereno, Development of diagnostic SCAR markers for *Meloidogyne graminicola, M. oryzae*, and *M. salasi* associated with irrigated rice fields in Americas, Plant Dis. 103 (2019) 83–88.
[3] E. Fanelli, A. Cotroneo, L. Carisio, A. Troccoli, S. Grosso, C. Boero, F. Capriglia, F. De Luca, Detection and molecular characterization of the rice root-knot nematode *Meloidogyne graminicola* in Italy, Eur. J. Plant Pathol. 149 (2017) 467–476.
[4] S. Mantelin, S. Bellafiore, T. Kyndt, *Meloidogyne graminicola*: a major threat to rice agriculture, Mol. Plant Pathol. 18 (2017) 3–15.
[5] A.-S. Masson, H.H. Bich, M. Simonin, H.N. Thi, P. Czernic, L. Moulin, S. Bellafiore, Deep modifications of the microbiome of rice roots infected by the parasitic nematode Meloidogyne graminicola in highly infested fields in Vietnam, FEMS (Fed. Eur. Microbiol. Soc.) Microbiol. Ecol. 96 (2020) fiaa099.
[6] A. Hada, T.K. Dutta, N. Singh, B. Singh, V. Rai, N.K. Singh, U. Rao, A genome-wide association study in Indian wild rice accessions for resistance to the root-knot nematode *Meloidogyne graminicola*, PLoS One 15 (2020) e0239085.
[7] D. Singh, T.K. Dutta, T.N. Shivakumara, M. Dash, H. Bollinedi, U. Rao, Suberin biopolymer in rice root exodermis reinforces preformed barrier against *Meloidogyne graminicola* infection, Rice Sci. 28 (2021) 301–312.
[8] R.H.C. Curtis, Plant-nematode interactions: Environmental signals detected by the nematode's chemosensory organs control changes in the surface cuticle and behaviour, Parasite 15 (2008) 310–316.
[9] A.M. Reynolds, T.K. Dutta, R.H.C. Curtis, S.J. Powers, H.S. Gaur, B.R. Kerry, Chemotaxis can take plant-parasitic nematodes to the source of a chemoattractant via the shortest possible routes, J. R. Soc. Interface 8 (2011) 568–577.
[10] P.K. Papolu, N.P. Gantasala, D. Kamaraju, P. Banakar, R. Sreevathsa, U. Rao, Utility of host delivered RNAi of two FMRFamide like peptides, *flp-14* and *flp-18*, for the management of root knot nematode, *Meloidogyne incognita*, PLoS One 8 (2013) e80603.
[11] P.K. Papolu, T.K. Dutta, A. Hada, D. Singh, U. Rao, The production of a synthetic chemodisruptive peptide *in planta* precludes *Meloidogyne incognita* multiplication in *Solanum melongena*, Physiol. Mol. Plant Pathol. 112 (2020) 101542.
[12] S. Rengarajan, E.A. Hallem, Olfactory circuits and behaviors of nematodes, Curr. Opin. Neurobiol. 41 (2016) 136–148.
[13] T.K. Dutta, P. Banakar, U. Rao, The status of RNAi-based transgenics in plant nematology, Front. Microbiol. 5 (2015) 760.
[14] R.N. Perry, Chemoreception in plant parasitic nematodes, Annu. Rev. Phytopathol. 34 (1996) 181–199.
[15] C.I. Bargmann, Chemosensation in *C. elegans. WormBook: the Online Review of C. elegans Biology*, 2006.
[16] T.N. Shivakumara, T.K. Dutta, S. Chaudhary, S.H. von Reuss, V.M. Williamson, U. Rao, Homologs of *Caenorhabditis elegans* chemosensory genes have roles in behaviour and chemotaxis in the root-knot nematode *Meloidogyne incognita*, Mol. Plant Microbe Interact. 32 (2019) 876–887.
[17] C. Kumari, T.K. Dutta, S. Chaudhary, P. Banakar, P.K. Papolu, U. Rao, Molecular characterization of FMRFamide-like peptides in *Meloidogyne graminicola* and analysis of their knockdown effect on nematode infectivity, Gene 619 (2017) 50–60.
[18] T.K. Dutta, V.S. Akhil, M. Dash, A. Kundu, V. Phani, A. Sirohi, Molecular and functional characterization of chemosensory genes from the root-knot nematode *Meloidogyne graminicola*, BMC Genom. 24 (2023) 745.
[19] R. Čepulytė, W.B. Danquah, G. Bruening, V.M. Williamson, Potent attractant for root-knot nematodes in exudates from seedling root tips of two host species, Sci. Rep. 8 (2018) 10847.
[20] N.T. Phan, J. Orjuela, E.G. Danchin, C. Klopp, L. Perfus-Barbeoch, D.K. Kozlowski, et al., Genome structure and content of the rice root-knot nematode (*Meloidogyne graminicola*), Ecol. Evol. 10 (2020) 11006–11021.
[21] V.S. Somvanshi, M. Dash, C.G. Bhat, R. Budhwar, J. Godwin, R.N. Shukla, A. Patrignani, R. Schlapbach, U. Rao, An improved draft genome assembly of *Meloidogyne graminicola* IARI strain using long-read sequencing, Gene 793 (2021) 145748.
[22] J. Chen, L. Hu, L. Sun, B. Lin, K. Huang, K. Zhuo, J. Liao, A novel *Meloidogyne graminicola* effector, MgMO237, interacts with multiple host defence-related proteins to manipulate plant basal immunity and promote parasitism, Mol. Plant Pathol. 19 (2018) 1942–1955.
[23] T.N. Shivakumara, P.K. Papolu, T.K. Dutta, D. Kamaraju, S. Chaudhary, U. Rao, RNAi-induced silencing of an effector confers transcriptional oscillation in another group of effectors in the root-knot nematode, *Meloidogyne incognita*, Nematology 18 (2016) 857–870.

[24] T.K. Dutta, S.J. Powers, B.R. Kerry, H.S. Gaur, R.H.C. Curtis, Comparison of host recognition, invasion, development and reproduction of *Meloidogyne graminicola* and *M. incognita* on rice and tomato, Nematology 13 (2011) 509–520.
[25] T.K. Dutta, P.K. Papolu, P. Banakar, D. Choudhary, A. Sirohi, U. Rao, Tomato transgenic plants expressing hairpin construct of a nematode protease gene conferred enhanced resistance to root-knot nematodes, Front. Microbiol. 6 (2015) 260.
[26] T.N. Shivakumara, T.K. Dutta, U. Rao, A novel *in vitro* chemotaxis bioassay to assess the response of *Meloidogyne incognita* towards various test compounds, J. Nematol. 50 (2018) 487–494.
[27] C.M. Zhang, N.H. Zhao, Y. Chen, D.H. Zhang, J.Y. Yan, W. Zou, K.Q. Zhang, X.W. Huang, The signaling pathway of *Caenorhabditis elegans* mediates chemotaxis response to the attractant 2-heptanone in a Trojan horse-like pathogenesis, J. Biol. Chem. 291 (2016) 23618–23627.
[28] C.M. Zhang, J.Y. Yan, Y. Chen, C.Y. Chen, K.Q. Zhang, X.W. Huang, The olfactory signal transduction for attractive odorants in *Caenorhabditis elegans*, Biotechnol. Adv. 32 (2014) 290–295.
[29] W. Cheng, H. Xue, X. Yang, D. Huang, M. Cai, F. Huang, L. Zheng, D. Peng, L.S. Thomashow, D.M. Weller, Z. Yu, J. Zhang, Multiple receptors contribute to the attractive response of *Caenorhabditis elegans* to pathogenic bacteria, Microbiol. Spectr. 11 (2023) e02319–e02322.
[30] Y. Yan, E.L. Davis, Characterisation of guanylyl cyclase genes in the soybean cyst nematode, *Heterodera glycines*, Int. J. Parasitol. 32 (2002) 65–72.
[31] Y. Li, Q. Ren, T. Bo, M. Mo, Y. Liu, AWA and ASH homologous sensing genes of *Meloidogyne incognita* contribute to the tomato infection process, Pathogens 11 (2022) 1322.
[32] S. Yu, L. Avery, E. Baude, D.L. Garbers, Guanylyl cyclase expression in specific sensory neurons: a new family of chemosensory receptors, Proc. Nat. Acad. Sci. U. S.A. 94 (1997) 3384–3387.
[33] P.N. Ng'ang'a, L. Siukstaite, A.E. Lang, H. Bakker, W. Römer, K. Aktories, G. Schmidt, Involvement of N-glycans in binding of *Photorhabdus luminescens* Tc toxin, Cell Microbiol. 23 (2021) e13326.
[34] L. Liu, Z. Li, X. Luo, X. Zhang, S.H. Chou, J. Wang, J. He, Which is stronger? A continuing battle between Cry toxins and insects, Front. Microbiol. 12 (2021) 665101.
[35] R.K. Sharma, T. Duda, C.L. Makino, Integrative signaling networks of membrane guanylate cyclases: biochemistry and Physiology, Front. Mol. Neurosci. 9 (2016) 83.
[36] D.M. Ferkey, P. Sengupta, N.D. L'Etoile, Chemosensory signal transduction in *Caenorhabditis elegans*, Genetics 217 (2021) iyab004.
[37] D.A. Fitzpatrick, D.M. O'Halloran, A.M. Burnell, Multiple lineage specific expansions within the guanylyl cyclase gene family, BMC Evol. Biol. 6 (2006) 26.
[38] I.N. Maruyama, Receptor guanylyl cyclases in sensory processing, Front. Endocrinol. 7 (2016) 173.
[39] D. Lazard, K. Zupko, Y. Poria, P. Net, J. Lazarovits, S. Horn, M. Khen, D. Lancet, Odorant signal termination by olfactory UDP glucuronosyl transferase, Nature 349 (1991) 790–793.
[40] F. Bozzolan, D. Siaussat, A. Maria, N. Durand, M.A. Pottier, T. Chertemps, M. Maïbèche-Coisne, Antennal uridine diphosphate (UDP)-glycosyltransferases in a pest insect: diversity and putative function in odorant and xenobiotics clearance, Insect Mol. Biol. 23 (2014) 539–549.
[41] S. Fraichard, A. Legendre, P. Lucas, I. Chauvel, P. Faure, F. Neiers, et al., Modulation of sex pheromone discrimination by a UDP-glycosyltransferase in *Drosophila melanogaster*, Genes 11 (2020) 237.
[42] M.L. Blaxter, P. De Ley, J.R. Garey, et al., A molecular evolutionary framework for the phylum Nematoda, Nature 392 (1998) 71–75.
[43] M. Holterman, A. van der Wurff, S. van den Elsen, H. van Megen, T. Bongers, O. Holovachov, J. Bakker, J. Helder, Phylum-wide analysis of SSU rDNA reveals deep phylogenetic relationships among nematodes and accelerated evolution toward crown clades, Mol. Biol. Evol. 23 (2006) 1792–1800.
[44] J.J. Dalzell, S. McMaster, M.J. Johnston, R. Kerr, C.C. Fleming, A.G. Maule, Non-nematode-derived double-stranded RNAs induce profound phenotypic changes in *Meloidogyne incognita* and *Globodera pallida* infective juveniles, Int. J. Parasitol. 39 (2009) 1503–1516.
[45] C.J. Lilley, L.J. Davies, P.E. Urwin, RNA interference in plant parasitic nematodes: a summary of the current status, Parasitology 139 (2012) 630–640.
[46] M.M. Sikder, M. Vestergård, Impacts of root metabolites on soil nematodes, Front. Plant Sci. 10 (2020) 1792.
[47] V. Vives-Peris, C. De Ollas, A. Gómez-Cadenas, R.M. Pérez-Clemente, Root exudates: from plant to rhizosphere and beyond, Plant Cell Rep. 39 (2020) 3–17.
[48] P. Sengupta, J.H. Chou, C.I. Bargmann, odr-10 encodes a seven transmembrane domain olfactory receptor required for responses to the odorant diacetyl, Cell 84 (1996) 899–909.
[49] P. Sengupta, H.A. Colbert, C.I. Bargmann, The *C. elegans* gene odr-7 encodes an olfactory-specific member of the nuclear receptor superfamily, Cell 79 (1994) 971–980.
[50] M.J. Wubben, H. Su, S.R. Rodermel, T.J. Baum, Susceptibility to the sugar beet cyst nematode is modulated by ethylene signal transduction in *Arabidopsis thaliana*, MPMI (Mol. Plant-Microbe Interact.) 14 (2001) 1206–1212.
[51] N. Wuyts, G. Lognay, M. Verscheure, M. Marlier, D. de Waele, R. Swennen, Potential physical and chemical barriers to infection by the burrowing nematode *Radopholus similis* in roots of susceptible and resistant banana (*Musa* spp.), Plant Pathol. 56 (2007) 878–890.
[52] N. Wuyts, R. Swennen, D. de Waele, Effects of plant phenylpropanoid pathway products and selected terpenoids and alkaloids on the behavior of the plant-parasitic nematodes *Radopholus similis, Pratylenchus penetrans* and *Meloidogyne incognita*, Nematology 8 (2006) 89–101.
[53] T.R. Fleming, A.G. Maule, C.C. Fleming, Chemosensory responses of plant parasitic nematodes to selected phytochemicals reveal long-term habituation traits, J. Nemat. 49 (2017) 462–471.